DVL3 Alleles Resulting in a −1 Frameshift of the Last Exon Mediate Autosomal-Dominant Robinow Syndrome

Janson J. White,[1,11] Juliana F. Mazzeu,[2,3,11] Alexander Hoischen,[4] Yavuz Bayram,[1] Marjorie Withers,[1] Alper Gezdirici,[5] Virginia Kimonis,[6] Marloes Steehouwer,[4] Shalini N. Jhangiani,[7] Donna M. Muzny,[7] Richard A. Gibbs,[1,7] Baylor-Hopkins Center for Mendelian Genomics, Bregje W.M. van Bon,[4] V. Reid Sutton,[1,8] James R. Lupski,[1,7,8,9] Han G. Brunner,[4,10,*] and Claudia M.B. Carvalho[1,*]

Robinow syndrome is a rare congenital disorder characterized by mesomelic limb shortening, genital hypoplasia, and distinctive facial features. Recent reports have identified, in individuals with dominant Robinow syndrome, a specific type of variant characterized by being uniformly located in the penultimate exon of *DVL1* and resulting in a −1 frameshift allele with a premature termination codon that escapes nonsense-mediated decay. Here, we studied a cohort of individuals who had been clinically diagnosed with Robinow syndrome but who had not received a molecular diagnosis from variant studies of *DVL1, WNT5A*, and *ROR2*. Because of the uniform location of frameshift variants in *DVL1*-mediated Robinow syndrome and the functional redundancy of DVL1, DVL2, and DVL3, we elected to pursue direct Sanger sequencing of the penultimate exon of *DVL1* and its paralogs *DVL2* and *DVL3* to search for potential disease-associated variants. Remarkably, targeted sequencing identified five unrelated individuals harboring heterozygous, de novo frameshift variants in *DVL3*, including two splice acceptor mutations and three 1 bp deletions. Similar to the variants observed in *DVL1*-mediated Robinow syndrome, all variants in *DVL3* result in a −1 frameshift, indicating that these highly specific alterations might be a common cause of dominant Robinow syndrome. Here, we review the current knowledge of these peculiar variant alleles in *DVL1*- and *DVL3*-mediated Robinow syndrome and further elucidate the phenotypic features present in subjects with *DVL1* and *DVL3* frameshift mutations.

Robinow syndrome is a genetically heterogeneous disorder that can segregate as either an autosomal-dominant (DRS1 [MIM: 180700]) or an autosomal-recessive (RRS [MIM: 268310]) trait. DRS can result from hypomorphic mutations in *WNT5A*[1,2] (MIM: 164975), whereas RRS is caused by biallelic loss-of-function variants in *ROR2*[3,4] (MIM: 602337). The original clinical description of Robinow syndrome included mesomelia, normal intellect, genital hypoplasia, and distinctive facial features comprising frontal bossing, prominent eyes, and a depressed nasal bridge, which are collectively referred to as a "fetal face."[5]

Recently, studies on cohorts of individuals presenting with DRS have identified an intriguing mutational mechanism, uniformly located frameshift mutations within *DVL1* (MIM: 601365), as a cause of DRS[6,7] (DRS2 [MIM: 616331]). The nature of these rare variants is remarkable: all cluster within the penultimate exon, consistently resulting in a −1 frameshift, and all share an identical premature termination codon. The mutant alleles are predicted to escape nonsense-mediated decay[8] (NMD) and thus result in a protein product containing a mutant C terminus that is rich in proline, highly basic, and greater than 100 amino acids in length.[6,7] However, a large fraction of individuals with DRS remain without an etiologic molecular diagnosis; they do not have variants in genes known to be associated with Robinow syndrome. It is noteworthy that all of the current known genic causes of Robinow syndrome, including heterozygous hypomorphic alleles in *WNT5A*, biallelic loss-of-function variants in *ROR2*, and frameshifts in *DVL1*, occur within genes involved in non-canonical Wnt signaling. *WNT5A* acts as an extracellular soluble ligand that is recognized by *ROR2*, and together they employ the dishevelled (DVL) family of proteins to further transduce the non-canonical signal.[9]

The complexity of human development requires coordination of distinct cellular signaling pathways. Core pathways, including hedgehog, TGF-β, and Wnt signaling, have been studied extensively. Wnt-β-catenin signaling consists of highly conserved machinery that coordinates cell fate, proliferation, and differentiation during development and tissue homeostasis.[10,11] Non-canonical, β-catenin-independent Wnt signaling is involved in orchestrating cell migration and tissue morphogenesis, including convergent-extension movements in vertebrate gastrulation.[12,13] Emerging data suggest that the

[1]Department of Molecular and Human Genetics, Baylor College of Medicine, Houston, TX 77030, USA; [2]Faculdade de Medicina, Universidade de Brasília, Brasília DF 70910900, Brazil; [3]Robinow Syndrome Foundation, Anoka, MN 55303, USA; [4]Department of Human Genetics, Radboud Institute for Molecular Life Sciences, Radboud University Nijmegen Medical Center, 6500 HB Nijmegen, the Netherlands; [5]Department of Medical Genetics, Kanuni Sultan Suleyman Training and Research Hospital, Istanbul 34303, Turkey; [6]Division of Genetics and Genomic Medicine, Department of Pediatrics, University of California, Irvine, Orange, CA 92868, USA; [7]Human Genome Sequencing Center, Baylor College of Medicine, Houston, TX 77030, USA; [8]Texas Children's Hospital, Houston, TX 77030, USA; [9]Department of Pediatrics, Baylor College of Medicine, Houston, TX 77030, USA; [10]Department of Clinical Genetics, Maastricht University Medical Center, 6202 AZ Maastricht, the Netherlands
[11]These authors contributed equally to this work
*Correspondence: han.brunner@radboudumc.nl (H.G.B.), cfonseca@bcm.edu (C.M.B.C.)
http://dx.doi.org/10.1016/j.ajhg.2016.01.005.

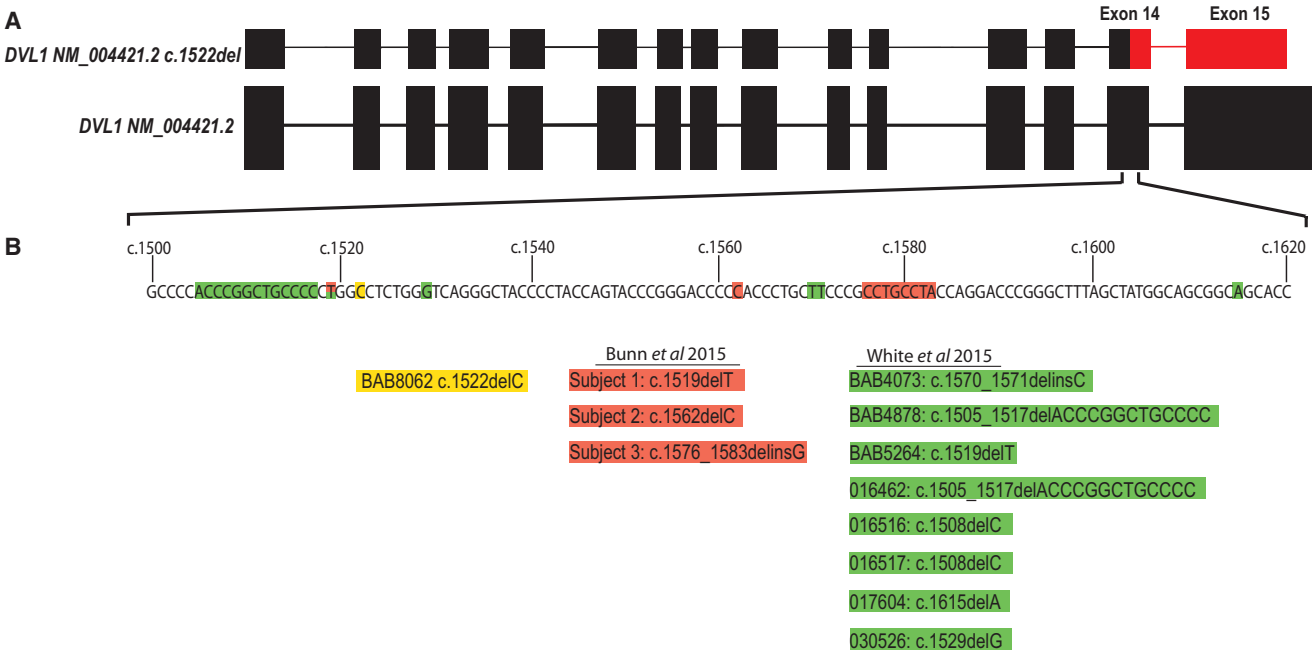

Figure 1. Locations of All Currently Described Variants Resulting in *DVL1*-Mediated Robinow Syndrome
(A) Depiction of the resulting mutant transcript in BAB8062. Black represent regions identical to the wild-type *DVL1*, and red indicates the mutant coding region.
(B) Locations of all variants currently described in the literature. Orange indicates nucleotides deleted in individuals reported by Bunn et al.,[6] green represents those from White et al.,[7] and yellow indicates those in BAB8062, reported here. All the variants are located within a stretch of ~110 nucleotides in the penultimate exon, and all are deletions that result in a −1 frameshift.

three human homologs of dishevelled, *DVL1*, *DVL2* (MIM: 602151), and *DVL3* (MIM: 601368), are core components in the correct routing and transmission of canonical and non-canonical Wnt signals, most likely by acting in large multiprotein complexes.[14,15] Collectively, Robinow syndrome appears to be a result of dysregulation in the WNT5A-ROR2-DVL pathway. Because a majority of individuals with Robinow syndrome do not receive a molecular diagnosis, we hypothesized that affected individuals have mutations residing in distinct genes within this branch of the non-canonical Wnt pathway, including the dishevelled human paralogs, *DVL1*, *DVL2*, and *DVL3*.

Because of the uniform location of disease-associated variants in *DVL1*-mediated Robinow syndrome and the knowledge that DVL1, DVL2, and DVL3 share 59%–67% amino acid homology,[16,17] we elected to perform direct Sanger sequencing of the penultimate and final exons of *DVL1*, *DVL2*, and *DVL3* in a cohort of 34 individuals referred to Radboud University Medical Center for diagnostic testing. All individuals had received a clinical diagnosis of possible Robinow syndrome by a clinical geneticist. DNA was obtained from the subjects and unaffected family members after they provided written informed consent. This study was approved by the Radboud University Medical Center review board and by the institutional review board at Baylor College of Medicine (protocol no. H-29697). Individuals were not pre-selected for similarity of their traits or possible modes of inheritance. From this cohort, 24 individuals had been screened for variants in *ROR2*, but no candidate variants were identified. *WNT5A* had been tested in one individual. Dominant inheritance was suspected for 16 individuals, and recessive inheritance was suspected in one individual. The mode of inheritance was undetermined for the remaining individuals. One individual from this large cohort, 015902, was found to have a frameshift deletion within the final exon of *DVL3*.

To confirm and assess the contribution of dishevelled to the phenotype, we then Sanger sequenced the penultimate and final exons of *DVL1*, *DVL2*, and *DVL3* from our in-house database of subjects (n = 17) with Robinow syndrome. These subjects were ascertained on the basis of clinical similarity to those with *DVL1*-mediated Robinow syndrome. Of the ten affected individuals, two were screened for variants in *WNT5A*, and two were screened for variants in *ROR2*. In concordance with the observations underlying *DVL1*-mediated Robinow syndrome,[7] one affected individual had a frameshift in the penultimate exon of *DVL1* (Figure 1). Remarkably, four additional individuals harbored variants in *DVL3*, including two frameshifts and two splice acceptor mutations affecting the penultimate or last exon (Figure 2). In total, one individual with a variant in *DVL1* and five individuals with variants in *DVL3* were identified from the above-described approach. All *DVL1* and *DVL3* variants identified from Sanger sequencing were annotated and analyzed with conceptual translation from Mutalyzer version 2.0.8.[18]

Individual BAB8062, who is of Turkish ancestry, harbored a de novo heterozygous 1 bp deletion in the penultimate

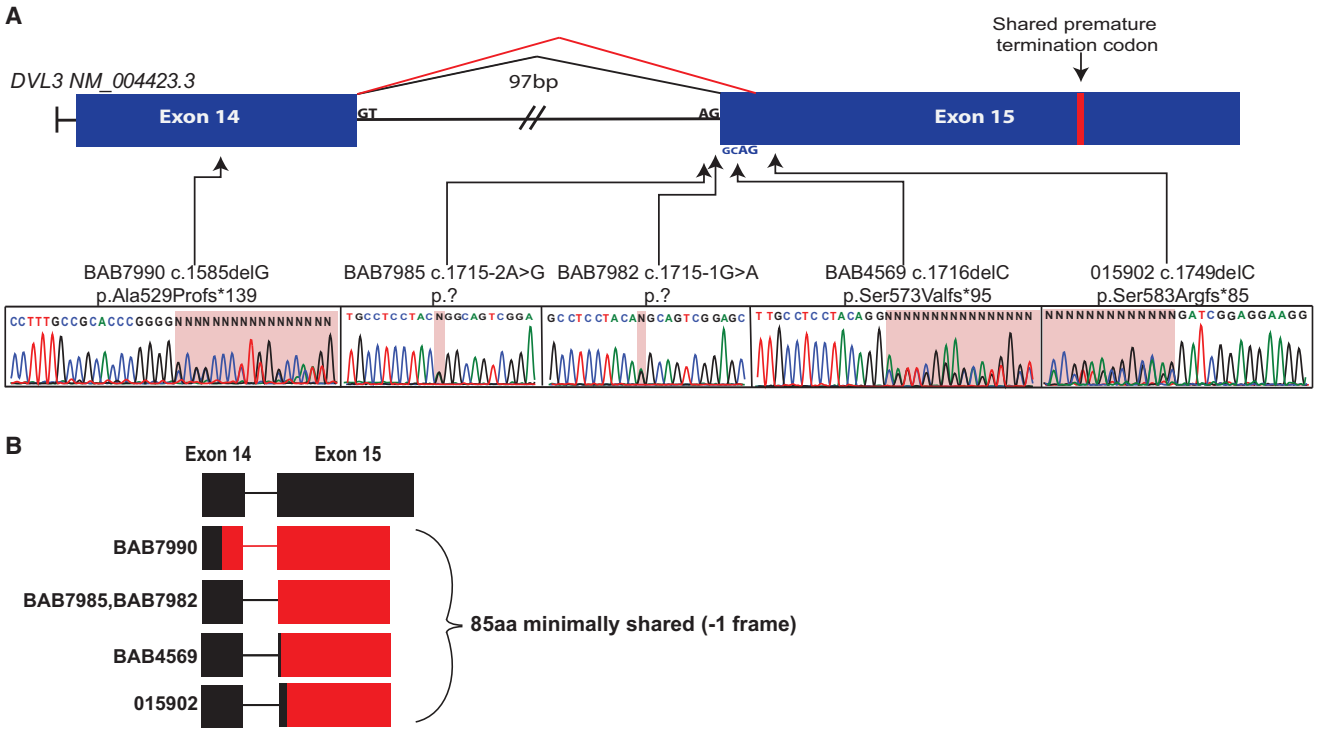

Figure 2. Robinow-Associated *DVL3* Variants
Overview of the variants identified in *DVL3* in individuals with autosomal-dominant Robinow syndrome.
(A) Location of the identified variants within the final two exons, including three frameshifts in coding regions and two splice acceptor variants. The red bar within exon 15 represents the shared premature termination codon of all individuals within our cohort.
(B) Representation of the predicted mutant C-terminal tail from Robinow-syndrome-affected individuals in our cohort. Black regions represent amino acids encoded by exons of the wild-type *DVL3*. Red regions represent mutant amino acids predicted to result from translation in the −1 frame.

exon of *DVL1*: c.1522delC (p.Pro508Leufs*141) (GenBank: NM_004421.2). To exclude the presence of this variant in other family members, we used standard PCR amplification. *DVL1* primer sequences consisted of 5′-GGG GAAGGGCAGGTAGGG-3′ (forward) and 5′-CAGTGAGT GGGGGCTTCG-3′ (reverse). Amplified PCR products were purified with ExoSAP-IT (Affymetrix) and sequenced with di-deoxynucleotide Sanger sequencing at the DNA Sequencing and Gene Vector Core at Baylor College of Medicine. The mutant allele was not observed in any family members, including the unaffected brother (BAB8065), unaffected mother (BAB8063), and unaffected father (BAB8064). In accordance with our previous observations for *DVL1*-mediated Robinow syndrome, this variant is located in the penultimate exon and is predicted to generate a premature termination codon within the last exon.

Figure 1 demonstrates the surprisingly uniform distribution of all previously reported *DVL1* variants found in subjects from four continents, including the variant identified in the Turkish subject (BAB8062) reported herein. Conceptual translation of the mutant allele in BAB8062 predicts that the variant will escape NMD and generate a C-terminally truncated protein from the −1 reading frame. The mutant allele is predicted to encounter a stop codon after the creation of a highly basic, proline-rich mutant C-terminal tail consisting of 140 amino acids while truncating the final 23 C-terminal amino acids. The presence of both mutant and wild-type mRNA in the lymphoblastoid cells from BAB8062 supports the hypothesis that the *DVL1* mutant transcript escapes NMD (Figure 3A). Furthermore, a TaqMan gene-expression assay of *DVL1* confirmed that the mutant allele's mRNA is expressed at levels similar to those in the unaffected parents (Figure 3B). These data are in agreement with previous reports[6,7] and further support the contention that *DVL1* −1 frameshift mutations that escape NMD are an important molecular cause of DRS.

Five individuals contained frameshift variants in *DVL3*, including two splice acceptor mutations and three 1 bp deletions; all of the identified variants are predicted to result in a frameshift to the −1 reading frame and a premature termination codon in the last exon. All identified variants in *DVL3* are represented in Figure 2 according to GenBank: NM_004423.3. Primers used to amplify the final two exons of *DVL3* were 5′-ACCACGGTCTCTCTCATCCA-3′ (forward) and 5′-AAGACGGACGGATGGAGAGA-3′ (reverse). BAB7990 harbored a frameshift deletion (c.1585delG [p.Ala529Profs*139]) located in the penultimate exon of *DVL3*, similar to the variants observed in *DVL1*. BAB4569 and 015902 contained 1 bp deletions located in the first several nucleotides of the final exon (c.1716delC [p.Ser573Valfs*95] and c.1749delC [p.Ser583Argfs*85], respectively). For confirming the resulting mutant reading

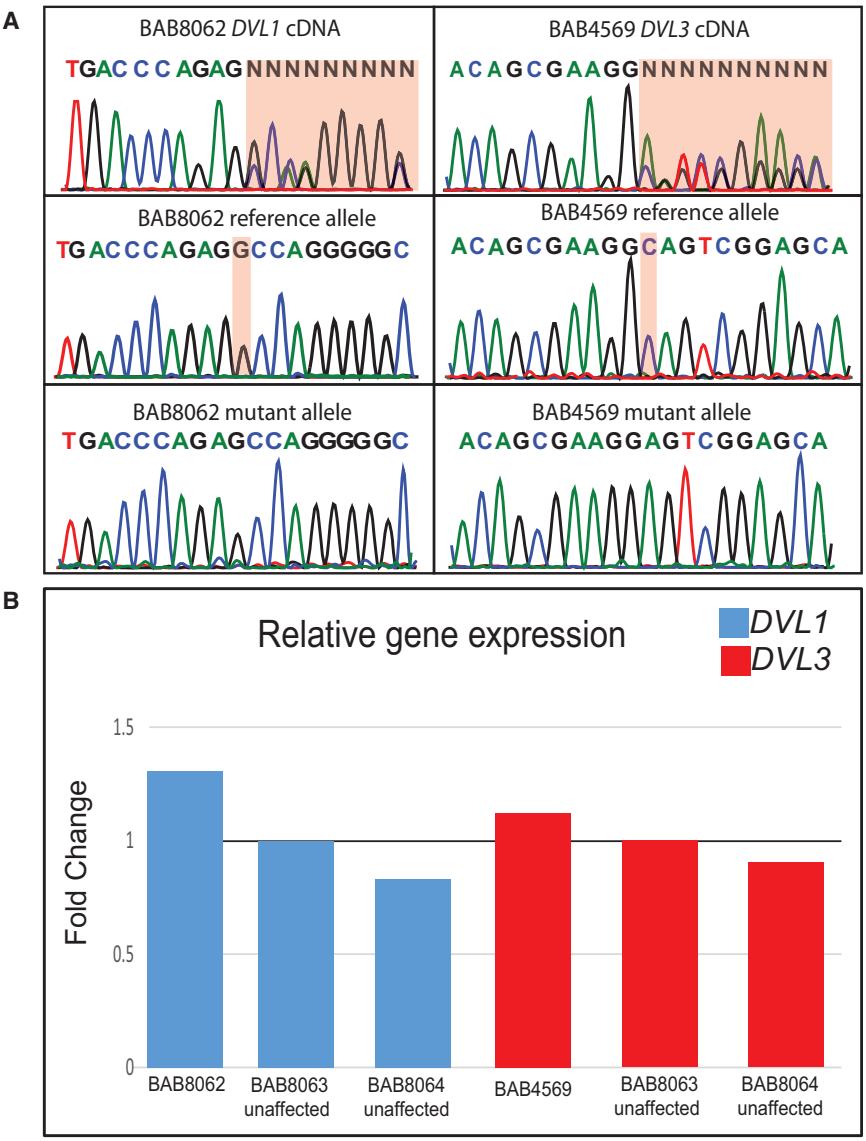

Figure 3. mRNA Expression of *DVL1* and *DVL3* Transcripts in Robinow Syndrome
(A) Chromatograms display Sanger sequencing results of cloned cDNA transcripts in BAB8062 (*DVL1*) and BAB4569 (*DVL3*). Mutant and reference alleles were cloned and sequenced independently for confirming mutant mRNA expression. (B) Depiction of the relative change in gene expression according to a TaqMan gene-expression assay for *DVL1* and *DVL3* with exon-spanning probes Hs00737028_m1 and Hs00610263_m1, respectively. For evaluating relative expression, the ΔΔct method[19] was used with *TBP* as the endogenous control and unaffected individual BAB8063 as the control subject.

frame, the frameshift deletions in BAB7990 and BAB4569 were manually cloned, and both alleles were sequenced independently. BAB4569 had previously undergone whole-exome sequencing as part of the Baylor-Hopkins Center for Mendelian Genomics initiative, but heterogeneous coverage, presumably due to poor capture resulting from high GC content of the region, prevented identification of this variant allele in our analytical informatics pipeline. Similar to those of *DVL1*, both mutant and wild-type transcripts of *DVL3* were expressed (Figure 3A) in carrier lymphoblastoid cell lines (BAB4569). In addition, *DVL3* did not show altered mRNA expression (Figure 3B). In aggregate, our data support the prediction that *DVL3* mutants escape NMD. Additionally, individuals BAB7982 and BAB7985 contained single-nucleotide variants (SNVs) in the canonical splice acceptor site of the final exon (c.1715−1G>A and c.1715−2A>G, respectively). In silico prediction of the splice-altering SNVs by the Human Splicing Finder[20] web tool predicts the activation of a cryptic splice acceptor site 2 bp downstream of the canonical splice acceptor site in both mutant transcripts. Activation of this cryptic splice site would result in the use of the −1 frame, which is predicted to create a mutant protein product similarly to all the observed *DVL3* variants reported herein. None of the described variants are reported in the 1000 Genomes Project, NHLBI Exome Sequencing Project, dbSNP, the Atherosclerosis Risk in Communities database of ~4,000 individuals, or our in-house database of >4,200 exomes, which include more than 600 individuals of Turkish ancestry. The identified Robinow-associated variants are not present in the Exome Aggregation Consortium (ExAC) Browser. However, analysis of the ExAC Browser indicated that three distinct frameshift indels are located in the 3′ coding region of *DVL3* and are predicted to escape NMD. Those variants have not been confirmed by Sanger sequencing. Furthermore, none of the alleles in the ExAC Browser create a protein product identical to those identified in our study.

Detailed clinical information was available for four subjects with Robinow syndrome due to *DVL3* frameshift alleles. The clinical phenotype of individuals harboring *DVL3* mutations is similar to that of individuals with *DVL1* mutations and concordant with earlier clinical descriptions of DRS (Table 1, Figure 4, Table S1; see Supplemental Data for detailed clinical descriptions).[21] Macrocephaly was found in two of four individuals with *DVL3* mutations and therefore cannot be used to distinguish between *DVL1*- and *DVL3*-mediated forms of Robinow syndrome. Curiously, two out of four individuals had telecanthus noted instead of true hypertelorism. Congenital heart defects and cleft lip and/or cleft palate, which can be a major

Table 1. Clinical Features of Individuals with *DVL3*-Mediated Robinow Syndrome

	Individuals[a]			
	BAB7990	**BAB7982**	**BAB4569**	**015902**
Current age	14 years	12 years	35 years	38 years
Age at last examination	10 years	19 months	33 years	27 years
Genotype	c.1585delG	c.1715−1G>A	c.1716delC	c.1749delC
De novo	affected father	+	+	affected mother
Gender	female	male	female	female
Growth Features				
Height percentile	$<3^{rd}$	$<3^{rd}$	$<3^{rd}$	$<3^{rd}$
Head-circumference percentile	50^{th}–75^{th}	50^{th}	$>98^{th}$	$>98^{th}$
Facial Features				
Frontal bossing	−	+	−	+
High forehead	−	+	−	−
Midface hypoplasia	+	+	+	+
Hypertelorism	+	+	−	−
Telecanthus	−	−	+	+
Upslanting palpebral fissures	+	+	−	+
Long eyelashes	+	+	−	−
Prominent eyes	+	+	+	−
Blue sclerae	+	ND	+	−
Epicanthal folds	−	ND	+	−
Anteverted nares	+	+	+	+
Wide, low nasal bridge	+	+	not low	+
Short nose	+	+	+	+
Long philtrum	+	−	+	+
Triangular mouth	−	−	+	−
Thin upper lip	−	−	−	−
Gingival hyperplasia	+	ND	+	+
Absent uvula	−	−	−	−
Cleft lip and/or palate	cleft palate	cleft lip and palate	cleft palate	−
Bilobed tongue	+ and short	ND	+	+
Dental anomalies	misaligned	ND	missing	missing
Short neck	−	−	−	webbed
Micrognathia	+	+	+	−
Abnormally shaped or positioned ears	−	low set	−	−
Skeletal Features				
Mesomelia	+	+	+	+
Brachydactyly	+	+	+	+
Clinodactyly	+	+	+	+
Syndactyly	+	−	−	−
Camptodactyly	+	−	−	−
Broad thumb	+	−	−	−

(*Continued on next page*)

Table 1. ***Continued***

	Individuals[a]			
	BAB7990	**BAB7982**	**BAB4569**	**015902**
Nail dysplasia	−	−	−	−
Bifid first and second phalanges	+	−	−	−
Hypoplastic phalanges	+	+ (fifth)	−	−
Broad first toe	+	−	−	+
Scoliosis or kyphosis	+	−	+	−
Pectus anomaly	+	ND	+	−
Urogenital Features				
Sacral dimple	+	−	−	−
Cryptorchidism	NA	+	NA	NA
Hypospadias	NA	−	NA	NA
Micropenis	NA	buried	NA	NA
Agenesis of the labia minora	−	NA	−	−
Small clitoris	+	NA	−	−
Urinary reflux	+	−	−	−
Inguinal hernia	−	−	−	−
Heart defects	VSD, PA, HRH	PDA, PFO, TR	VSD	−
Umbilical hernia	−	−	−	+
Seizures	−	−	−	−
Hearing loss	−	−	+	−
Omphalocele	+	−	−	−
Hepatomegaly	−	−	−	−

Abbreviations are as follows: +, present; −, absent; NA, not applicable; ND, no data; PA, pulmonary atresia; HRH, hypoplastic right heart; PDA, patent ductus arteriosus; PFO, patent foramen ovale; TR, tricuspid regurgitation; and VSD, ventricular septal defect.
[a]Clinical data were not available for subject BAB7985.

clinical-management concern at birth, were observed in three out of four individuals. It is noteworthy that all individuals with *DVL3* mutations have short stature, whereas individuals with *DVL1* mutations have a final stature in the low-normal range.[7] None of the individuals with *DVL3* variants have been reported to have osteosclerosis, but no specific investigation was conducted to exclude it.

Dishevelled (*dsh*), originally discovered in *Drosophila melanogaster*, is necessary for tissue patterning. *Drosophila dsh* has evolved three mammalian orthologs: the homologous genes *DVL1*, *DVL2*, and *DVL3*. Our data support the growing evidence that fly genes with greater than one human homolog are more likely to be associated with human Mendelian diseases than are fly genes with a single human homolog, indicating possible specialization during evolution.[22] In mice, DVL1 and DVL3 co-localize within the developing neural tube, and all three DVL proteins have similar localization patterns.[23] Whereas $Dvl1^{-/-}$ mice have a mild phenotype including social abnormalities, $Dvl2^{-/-}$ and $Dvl3^{-/-}$ mice independently demonstrate partial lethality and conotruncal defects. Double knockout of either *Dvl1* and *Dvl2* or *Dvl2* and *Dvl3* results in neural-tube defects, suggesting redundant roles between the DVL homologs.[24] However, $Dvl1^{-/-}Dvl3^{-/-}$ mice do not display neural-tube defects, indicating functional divergence between the DVL homologs;[24,25] one study has estimated that DVL2 contributes more than 95% of the total DVL pool in several mouse cell types.[26]

Our data strongly support previous studies reporting that specific −1 frameshift variants in the penultimate exon of *DVL1* cause autosomal-dominant Robinow syndrome. The current literature available on *DVL1*-mediated Robinow syndrome indicates that these variants are highly specific and tightly cluster in the penultimate exon and lead to a mutant C-terminal peptide tail that is highly basic and proline rich (Figure 1). Our data from a subject of Turkish origin, with the same clinically recognizable specific diagnosis of Robinow syndrome, further support the notion that *DVL1*-mediated Robinow syndrome is a product of the mutant C-terminal tail, a direct result of −1 frameshift variants, and causes the mutant DVL1 to act in a dominant-negative or gain-of-function manner.

As a result of the high similarity among paralogous DVLs, DVL1, DVL2, and DVL3 in mice and humans have

Figure 4. Facial Features of the Individuals with DRS in This Study
Individuals BAB4569, BAB7982, BAB7990, and 015902 have *DVL3* variants, and BAB8062 has a de novo variant in *DVL1*.

been proposed to have functional redundancy.[24,27,28] All variants observed thus far to underly DVL-mediated Robinow syndrome result in a mutant C-terminal tail, the presence of which most likely alters protein folding, potentially affecting numerous C-terminal phosphorylation sites and obstructing C-terminal interactors. The three DVL homologs are capable of forming large dynamic multiprotein complexes observed as cellular puncta,[14] and these self-associated forms of DVL are critical for its role in signaling the canonical pathway.[15] The self-associated DVL puncta can be dispersed by the hyperphosphorylation of DVL. Casein kinase 1ε (CK1ε) is the major kinase responsible for Wnt-induced DVL3 phosphorylation.[29] Interestingly, the hyperphosphorylation of DVL3 requires C-terminal serine clusters, the absence of which alters the DVL3 subcellular localization and DVL polymerization.[29] It is possible that the C termini of DVLs have an ability to suppress canonical Wnt-β-catenin signaling and promote non-canonical Wnt transduction. Therefore, DVL-mediated Robinow syndrome might be a result of specific mutations that affect the phosphorylation of the C-terminal tails of DVL1 and DVL3. Further evidence of this is supported by the interaction between phosphorylated DVL3 and the non-canonical Wnt receptor ROR2.[30] Stimulated by the hyperphosphorylation of DVL3 by CK1ε, ROR2 has been shown to interact with DVL3. Interestingly, the DVL3-ROR2 interaction is dependent on the DVL C terminus, which is lost in all observed DVL mutants we have identified thus far.[31] Curiously, a *DVL1* truncated allele was observed to increase canonical signaling only when co-expressed in an equal ratio with the wild-type *DVL1*[6] in vitro, perhaps indicating a dominant-negative interaction given the regulated stoichiometry between the homologs of DVL within the large signaling complex and its dynamic polymerization, which might be partially regulated by ROR2.[30] Further work is necessary to elucidate the mechanism by which these specific mutations in *DVL1* and *DVL3* result in DRS and their interactions within the global Wnt signalosome.

We conclude that Sanger sequencing of the penultimate and final exons of *DVL1* and *DVL3* in individuals with a suspected diagnosis of autosomal-dominant Robinow syndrome is a prudent means for potentially establishing a molecular diagnosis. In addition to identifying truncating variants in *DVL3* as a cause of Robinow syndrome, we have shown that these parallel the distinct −1 frameshift mutational mechanism elucidated in *DVL1*-mediated Robinow syndrome. Additionally we have shown that the phenotypic features of *DVL1*- and *DVL3*-mediated Robinow syndrome are largely concordant, but possible distinguishing features include head circumference and stature. Clinical investigations of subjects with Robinow syndrome are required for exploring the associated increased bone mineral density and the potential underlying Wnt-signaling differences related to bone mineralization.

Accession Numbers

The accession number for the whole-exome sequencing DNA sequences reported in this paper is dbGaP: phs000711, under the Baylor Hopkins Center for Mendelian Genomics study. Sample identifiers are SRS915722, SRS915721, and SRS915720. Additionally, the accession numbers for all variants identified in *DVL1* and *DVL3* are ClinVar: SCV000257455, SCV000257456, SCV000257457, SCV000257458, SCV000257459, and SCV000257460.

Supplemental Data

Supplemental Data include one table and a Supplemental Note and can be found with this article online at http://dx.doi.org/10.1016/j.ajhg.2016.01.005.

Conflicts of Interest

J.R.L. holds stock ownership in 23andMe Inc. and Lasergen Inc., is a paid consultant for Regeneron Pharmaceuticals, and is a co-inventor on multiple United States and European patents related to molecular diagnostics. The Department of Molecular and Human Genetics at Baylor College of Medicine derives revenue from molecular genetic testing offered in the Baylor-Miraca Medical Genetics Laboratories (BMGL). J.R.L. is on the Scientific Advisory Board of the BMGL.

Acknowledgments

This work was supported in part by the Baylor Hopkins Center for Mendelian Genomics (U54HG006542), jointly funded by the National Human Genome Research Institute (NHGRI) and National Heart, Lung, and Blood Institute (NHLBI). J.J.W. is funded in part by the Smith-Magenis Syndrome Research Foundation. The content is solely the responsibility of the authors and does not necessarily represent the official views of the NHGRI, NHLBI, or NIH. The authors would like to thank the Exome Aggregation Consortium and the groups that provided exome variant data for comparison. A full list of contributing groups can be found at http://exac.broadinstitute.org/about.

Received: October 8, 2015
Accepted: January 19, 2016
Published: February 25, 2016

Web Resources

The URLs for data presented herein are as follows:

1000 Genomes, http://www.1000genomes.org
Atherosclerosis Risk in Communities Study, http://www2.cscc.unc.edu/aric
Baylor Miraca Genetics Laboratories, http://www.bcm.edu/geneticlabs/
Clinvar, http://www.ncbi.nlm.nih.gov/clinvar/
dbGaP, http://www.ncbi.nlm.nih.gov/gap
Exome Aggregation Consortium (ExAC) Browser, http://exac.broadinstitute.org
NHLBI Exome Sequencing Project (ESP) Exome Variant Server, http://www.evs.gs.washington.edu/EVS
OMIM, http://www.omim.org
RefSeq, http://www.ncbi.nlm.nih.gov/refseq/

References

1. Person, A.D., Beiraghi, S., Sieben, C.M., Hermanson, S., Neumann, A.N., Robu, M.E., Schleiffarth, J.R., Billington, C.J., Jr., van Bokhoven, H., Hoogeboom, J.M., et al. (2010). WNT5A mutations in patients with autosomal dominant Robinow syndrome. Dev. Dyn. *239*, 327–337.
2. Roifman, M., Marcelis, C.L.M., Paton, T., Marshall, C., Silver, R., Lohr, J.L., Yntema, H.G., Venselaar, H., Kayserili, H., van Bon, B., et al.; FORGE Canada Consortium (2015). De novo WNT5A-associated autosomal dominant Robinow syndrome suggests specificity of genotype and phenotype. Clin. Genet. *87*, 34–41.
3. Afzal, A.R., Rajab, A., Fenske, C.D., Oldridge, M., Elanko, N., Ternes-Pereira, E., Tüysüz, B., Murday, V.A., Patton, M.A., Wilkie, A.O., and Jeffery, S. (2000). Recessive Robinow syndrome, allelic to dominant brachydactyly type B, is caused by mutation of ROR2. Nat. Genet. *25*, 419–422.
4. van Bokhoven, H., Celli, J., Kayserili, H., van Beusekom, E., Balci, S., Brussel, W., Skovby, F., Kerr, B., Percin, E.F., Akarsu, N., and Brunner, H.G. (2000). Mutation of the gene encoding the ROR2 tyrosine kinase causes autosomal recessive Robinow syndrome. Nat. Genet. *25*, 423–426.
5. Robinow, M., Silverman, F.N., and Smith, H.D. (1969). A newly recognized dwarfing syndrome. Am. J. Dis. Child. *117*, 645–651.
6. Bunn, K.J., Daniel, P., Rösken, H.S., O'Neill, A.C., Cameron-Christie, S.R., Morgan, T., Brunner, H.G., Lai, A., Kunst, H.P.M., Markie, D.M., and Robertson, S.P. (2015). Mutations in DVL1 cause an osteosclerotic form of Robinow syndrome. Am. J. Hum. Genet. *96*, 623–630.
7. White, J., Mazzeu, J.F., Hoischen, A., Jhangiani, S.N., Gambin, T., Alcino, M.C., Penney, S., Saraiva, J.M., Hove, H., Skovby, F., et al.; Baylor-Hopkins Center for Mendelian Genomics (2015). DVL1 frameshift mutations clustering in the penultimate exon cause autosomal-dominant Robinow syndrome. Am. J. Hum. Genet. *96*, 612–622.
8. Khajavi, M., Inoue, K., and Lupski, J.R. (2006). Nonsense-mediated mRNA decay modulates clinical outcome of genetic disease. Eur. J. Hum. Genet. *14*, 1074–1081.
9. Oishi, I., Suzuki, H., Onishi, N., Takada, R., Kani, S., Ohkawara, B., Koshida, I., Suzuki, K., Yamada, G., Schwabe, G.C., et al. (2003). The receptor tyrosine kinase Ror2 is involved in non-canonical Wnt5a/JNK signalling pathway. Genes Cells *8*, 645–654.
10. Clevers, H. (2006). Wnt/β-catenin signaling in development and disease. Cell *127*, 469–480.
11. MacDonald, B.T., Tamai, K., and He, X. (2009). Wnt/β-catenin signaling: components, mechanisms, and diseases. Dev. Cell *17*, 9–26.
12. Yamanaka, H., Moriguchi, T., Masuyama, N., Kusakabe, M., Hanafusa, H., Takada, R., Takada, S., and Nishida, E. (2002). JNK functions in the non-canonical Wnt pathway to regulate convergent extension movements in vertebrates. EMBO Rep. *3*, 69–75.
13. Sokol, S. (2000). A role for Wnts in morpho-genesis and tissue polarity. Nat. Cell Biol. *2*, E124–E125.
14. Yokoyama, N., Golebiewska, U., Wang, H.Y., and Malbon, C.C. (2010). Wnt-dependent assembly of supermolecular Dishevelled-3-based complexes. J. Cell Sci. *123*, 3693–3702.
15. Schwarz-Romond, T., Fiedler, M., Shibata, N., Butler, P.J.G., Kikuchi, A., Higuchi, Y., and Bienz, M. (2007). The DIX domain of Dishevelled confers Wnt signaling by dynamic polymerization. Nat. Struct. Mol. Biol. *14*, 484–492.
16. Pizzuti, A., Amati, F., Calabrese, G., Mari, A., Colosimo, A., Silani, V., Giardino, L., Ratti, A., Penso, D., Calzà, L., et al. (1996). cDNA characterization and chromosomal mapping of two human homologues of the Drosophila dishevelled polarity gene. Hum. Mol. Genet. *5*, 953–958.
17. Semënov, M.V., and Snyder, M. (1997). Human dishevelled genes constitute a DHR-containing multigene family. Genomics *42*, 302–310.
18. Wildeman, M., van Ophuizen, E., den Dunnen, J.T., and Taschner, P.E. (2008). Improving sequence variant descriptions in mutation databases and literature using the Mutalyzer sequence variation nomenclature checker. Hum. Mutat. *29*, 6–13.

19. Livak, K.J., and Schmittgen, T.D. (2001). Analysis of relative gene expression data using real-time quantitative PCR and the 2(-Delta Delta C(T)) Method. Methods *25*, 402–408.
20. Desmet, F.O., Hamroun, D., Lalande, M., Collod-Béroud, G., Claustres, M., and Béroud, C. (2009). Human Splicing Finder: an online bioinformatics tool to predict splicing signals. Nucleic Acids Res. *37*, e67.
21. Mazzeu, J.F., Pardono, E., Vianna-Morgante, A.M., Richieri-Costa, A., Ae Kim, C., Brunoni, D., Martelli, L., de Andrade, C.E., Colin, G., and Otto, P.A. (2007). Clinical characterization of autosomal dominant and recessive variants of Robinow syndrome. Am. J. Med. Genet. A. *143*, 320–325.
22. Yamamoto, S., Jaiswal, M., Charng, W.L., Gambin, T., Karaca, E., Mirzaa, G., Wiszniewski, W., Sandoval, H., Haelterman, N.A., Xiong, B., et al. (2014). A drosophila genetic resource of mutants to study mechanisms underlying human genetic diseases. Cell *159*, 200–214.
23. Wang, J., Hamblet, N.S., Mark, S., Dickinson, M.E., Brinkman, B.C., Segil, N., Fraser, S.E., Chen, P., Wallingford, J.B., and Wynshaw-Boris, A. (2006). Dishevelled genes mediate a conserved mammalian PCP pathway to regulate convergent extension during neurulation. Development *133*, 1767–1778.
24. Etheridge, S.L., Ray, S., Li, S., Hamblet, N.S., Lijam, N., Tsang, M., Greer, J., Kardos, N., Wang, J., Sussman, D.J., et al. (2008). Murine dishevelled 3 functions in redundant pathways with dishevelled 1 and 2 in normal cardiac outflow tract, cochlea, and neural tube development. PLoS Genet. *4*, e1000259.
25. Lijam, N., Paylor, R., McDonald, M.P., Crawley, J.N., Deng, C.-X., Herrup, K., Stevens, K.E., Maccaferri, G., McBain, C.J., Sussman, D.J., and Wynshaw-Boris, A. (1997). Social interaction and sensorimotor gating abnormalities in mice lacking Dvl1. Cell *90*, 895–905.
26. Lee, Y.N., Gao, Y., and Wang, H.Y. (2008). Differential mediation of the Wnt canonical pathway by mammalian Dishevelleds-1, -2, and -3. Cell. Signal. *20*, 443–452.
27. Hamblet, N.S., Lijam, N., Ruiz-Lozano, P., Wang, J., Yang, Y., Luo, Z., Mei, L., Chien, K.R., Sussman, D.J., and Wynshaw-Boris, A. (2002). Dishevelled 2 is essential for cardiac outflow tract development, somite segmentation and neural tube closure. Development *129*, 5827–5838.
28. Wang, H.Y., and Malbon, C.C. (2012). Dishevelled C-terminus: prolyl and histidinyl motifs. Acta Physiol. (Oxf.) *204*, 65–73.
29. Bernatík, O., Šedová, K., Schille, C., Ganji, R.S., Červenka, I., Trantírek, L., Schambony, A., Zdráhal, Z., and Bryja, V. (2014). Functional analysis of dishevelled-3 phosphorylation identifies distinct mechanisms driven by casein kinase 1ϵ and frizzled5. J. Biol. Chem. *289*, 23520–23533.
30. Nishita, M., Itsukushima, S., Nomachi, A., Endo, M., Wang, Z., Inaba, D., Qiao, S., Takada, S., Kikuchi, A., and Minami, Y. (2010). Ror2/Frizzled complex mediates Wnt5a-induced AP-1 activation by regulating Dishevelled polymerization. Mol. Cell. Biol. *30*, 3610–3619.
31. Witte, F., Bernatik, O., Kirchner, K., Masek, J., Mahl, A., Krejci, P., Mundlos, S., Schambony, A., Bryja, V., and Stricker, S. (2010). Negative regulation of Wnt signaling mediated by CK1-phosphorylated Dishevelled via Ror2. FASEB J. *24*, 2417–2426.

The American Journal of Human Genetics, Volume *98*

Supplemental Information

DVL3 Alleles Resulting in a −1 Frameshift of the Last Exon Mediate Autosomal-Dominant Robinow Syndrome

Janson J. White, Juliana F. Mazzeu, Alexander Hoischen, Yavuz Bayram, Marjorie Withers, Alper Gezdirici, Virginia Kimonis, Marloes Steehouwer, Shalini N. Jhangiani, Donna M. Muzny, Richard A. Gibbs, Bregje W.M. van Bon, V. Reid Sutton, James R. Lupski, Han G. Brunner, Claudia M.B. Carvalho, and Baylor-Hopkins Center for Mendelian Genomics

Table S1. Phenotypic features of *DVL1*-mediated Robinow syndrome

	Citation	**Current**	**White et al (2015) *Am J Hum Genet 96*:612-622**								TOTAL
	Individual ID	BAB8062	BAB4073	BAB4878	BAB5264	016462	016516	016517	017604	030526	
	Current age	1yr	11 yr	22 yr	6 yr	20 yr	21 yr	21 yr	15yr 6 ms	42	
	Genotype	c.1522delC	c.1570_1571delinsC	c.1505_1517del ACCCGGCTGCCC	c.1519delT	c.1505_1517del ACCCGGCTGCCC	c.1508delC	c.1508delC	c.1615del	c.1529delA	
	De novo	+	+	+	NA	+	+	+	+	NA	
	Gender	M	F	F	M	F	M	M	M	F	
Growth	Height percentile	<3%	10%	17%	<3%	70%	90%	75%	80%	<3%	
	OFC SD	ND	+4 SD	+2.5 SD	>+2 SD	>+4 SD	>+4 SD	>+4 SD	>+4SD	> +6 SD	
Facial features	Macrocephaly	+	+	+	+	+	+	+	+	+	9/9
	Frontal bossing	+	+	+	+	+	+	+	+	+	9/9
	Hypertelorism	+	+	+	+	+	+	+	+	+	12/12
	Upslanting palpebral fissures	+	+	+	-	ND	-	-	-	-	3/9
	Prominent eyes	+	+	-	+	ND	+	+	-	+	6/8
	Anteverted nares	+	+	+	+	+	+	+	-	ND	7/8
	Depressed nasal bridge	+	+	+	+	ND	+	+	+	+	10/10
	Short nose	+	+	+	+	+	+	+	+	+	11/11
	Gingival hyperplasia	+	+	+	+	+	+	+	+	-	10/12
	Cleft soft palate	+	+	-	-	ND	-	-	-	-	4/11
	Dental anomalies	+	+	+	+	+	+	+	+	+	12/12
	Micrognathia	+	+	-	+	+	-	-	-	-	4/9
Skeletal	Mesomelia	+	+	+	+	+	+	+	+	+	9/9
	Brachydactyly	+	+	+	+	+	+	+	-	+	10/12
	Clinodactyly	+	+	+	+	+	-	-	+	+	7/9
	Bifid phalanges	-	-	-	-	ND	+	+	ND	-	4/9
	Scoliosis or kyphosis	+	-	-	-	+	-	-	+	+	4/10
	Pectus anomaly	+	+	+	-	ND	+	+	+	-	7/9
	Increased bone density (skull)	+	ND	+	ND	+	-	-	+	ND	7/9
Other features	Hearing loss	-	-	-	+	+	-	-	-	+	3/9
	Sacral dimple	+ (+dimple between scrotum and anus)	+	-	ND	ND	-	-	-	-	3/9
	Absent anterior nasal spine	+	-	-	-	+	-	-	-	+	3/9

Abbreviations are as follows: +, Present; -, Absent; F, Female; M, Male; ND, No data; NA, Not available; OFC, Occipitofrontal Circumference.

Supplemental Note: Case reports

BAB7990

BAB 7990 is a female patient born from a healthy mother and an affected father. She was born with omphalocele, short gut, multiple congenital heart defects (hypoplastic right heart, ventricular septum defect (VSD), pulmonary atresia), chronic lung disease with tracheomalacia and cleft palate, requiring multiple surgeries and a tracheostomy. She was developmentally delayed presumed to be due to multiple medical interventions. She walked at age 3y and spoke at age 5y. She is intellectually normal and attends regular school at the age appropriate grade. Clinical examination at age 10y noted short stature, midface hypoplasia, short neck, prominent eyes, upslanted palpebral fissures, long eyelashes, hypertelorism, bushy eyebrows, short nose with anteverted nares, long philtrum, downslanted mouth corners, bifid short tongue, gingival hyperplasia, dental malalignment, anteriorized anus, single palmar crease on the left hand, large duplicated thumb, camptodactyly, syndactyly. Upon physical evaluation she displayed mesomelia with both upper and middle arm segments below 5th centile, more pronounced in the middle segment. She has pectus excavatum and urinary reflux. Sanger sequencing did not show *DVL1* mutations.

Father of BAB7990

BAB 7990 (Father) is a male patient born from a non-consanguineous healthy couple. He was examined by us at age 33. Clinical examination noted short stature (3rd centile), midface hypoplasia, epicanthal folds, long eyelashes, upslanted palpebral fissures, hypertelorism, wide nasal bridge, short and wide nose, anteverted nares, long philtrum, downturned mouth corners, cleft lip and palate, bifid tongue, microretrognathia and dental malocclusion. His arms have mildly mesomelic shortening. He has brachydactyly, large thumbs, clinodactyly, large halluces, pectus excavatum. He was born with omphalocele.

He was diagnosed with Robinow syndrome just after his daughter's birth. He has yet to be tested for *DVL3* mutations.

BAB4569

She was born by C-section at 40 weeks of gestation from non-consanguineous parents and had no major problems during the neonatal period. She has a fraternal female twin. Though her development was normal she had physical and speech therapy. She walked at 15 months and spoke at 18 months. She graduated college as a nurse. Clinical examination at age 25 years old revealed that she weighed 62kg (<75^{th} centile), height 144 cm (<3^{rd} centile). She displayed mesomelia based on physical evaluation with forearm <5^{th} centile and arm $5^{th-10th}$ centile. She has only 22 permanent teeth and had a submucous cleft palate. She was born with a VSD. She has bilateral cataracts and 50% unilateral hearing loss. She underwent breast reduction surgery, and had cystic ovaries and had premature menopause. Her genitalia were referred to as normal. She was screened for mutations in *WNT5*A and no mutations were found. Whole exome sequencing did not show variants in *WNT5A* or *ROR2*.

015902

015902 is a female patient born from a non-consanguineous couple. At clinical examination at age 27y she is obese, has short stature, macrocephaly (>98^{th} centile), midface hypoplasia, upslanted palpebral fissures, hypertelorism, downturned mouth corners, bifid tongue, gingival hyperplasia, retrognathia, webbed neck. She has several missing teeth. Examination was performed after facial esthetical surgeries. She has mesomelic limb shortening, short hands, brachydactyly, large halluces and a sandal gap by physical evaluation. The mother is reported to have a similar phenotype but she was not examined or tested. Screening of *WNT5A* and *DVL1* identified no pathogenic variants.

BAB7982

BAB 7982 is a 12 year old male patient born from non-consanguineous healthy parents. At birth he presented with cleft lip and palate, undescended testicles, persistent ductus arteriosus (PDA), patent foramen ovale (PFO) and tricuspid regurgitation. On physical examination at age 13 months he had short stature (length 3rd centile), frontal bossing, broad nasal root, hypertelorism, short nose with anteverted nares, low placed ears, gingival hyperplasia, micrognathia, widely spaced nipples, rhizomelic limb shortening, broad and wide fingers, 5th finger clinodactyly. Radiographic evaluation revealed mesomelia. His penis was buried but of normal size and he had left cryptorchidism (previous orchidopexy of the right testicle).

BAB8062

The proband is a 13-month-old Turkish male patient who was born to a 27 years old G4P2 healthy mother after an uncomplicated pregnancy and delivery with a birth weight of 3020g (10^{th} centile) and birth length of 42 cm ($<3^{rd}$ centile) (occipitofrontal circumference not available). The mother`s first and second pregnancies were terminated at 8 weeks of gestation due to undetected fetal cardiac activity. The patient was admitted to the neonatal intensive care unit after delivery for 11 days because of antenatally detected cleft lip and palate and ambiguous genitalia. Because of the ambiguous genitalia the levels of 17-OH progesterone, 4-androstenedione, cortisol, and testosterone were tested and found to be normal. Chromosome analysis also revealed a normal 46,XY karyotype. He underwent right unilateral inguinal hernia and orchidopexy at 4 months of age and cleft lip and palate surgery at 7 months of age. He was able to hold his head at 4.5 months of age and sit unsupported at 11 months of age.

He was referred to the genetics clinic at age 13 months because of short stature and dysmorphic features. The anthropometric measures at that age were 9000 g (10-25 centile) body weight, 73.5 cm (3-10^{th} centile) height, and 49 cm (90^{th} centile)

occipitofrontal circumference. On head and neck examination relative macrocephaly, large anterior fontanelle (2x2 cm), frontal bossing, wide and high forehead, mid-face hypoplasia, prominent eyes, hypertelorism, blue sclerae, epicanthal folds, telecanthus, broad nasal root, short nose, aplasia of the uvula, dental anomalies secondary to cleft lip and palate, gingival hyperplasia, micrognathia, low-set and question mark shaped ears, and short neck were detected. On skeletal system examination, mesomelic shortening of limbs, brachydactyly, clinodactyly of 5^{th} fingers, broad thumbs, nail hypoplasia, and prominent left 12^{th} costovertebral region. Genitourinary system examination revealed non-palpable testes, micropenis, hypospadias, sacral dimple, and dimple on pelvic floor (between scrotum and anus). On neurologic examination he was not able to walk unsupported and there was no speech. X-ray survey showed hyperostosis of the skull base (especially at the sella turcica), flattened vertebral bodies (platyspondyly), kyphoscoliosis, and bilateral developmental dysplasia of the hip. On scrotal ultrasound right testis (16x7 mm) was viewed in inguinal canal and left testis (11x8 mm) was viewed in lower left abdomen. A clinical diagnosis of Robinow syndrome was rendered.